AD-A083 659 BROWN UNIV PROVIDENCE R I DIV OF ENGINEERING F/G 20/6
REMOTE OPTICAL CONTROL AND SWITCHING IN OPTICAL FIBER LINKS.(U)
JAN 80 R V GAUTHIER, A V NURMIKKO F19628-78-C-0009
UNCLASSIFIED RADC -TR-79-346 NL

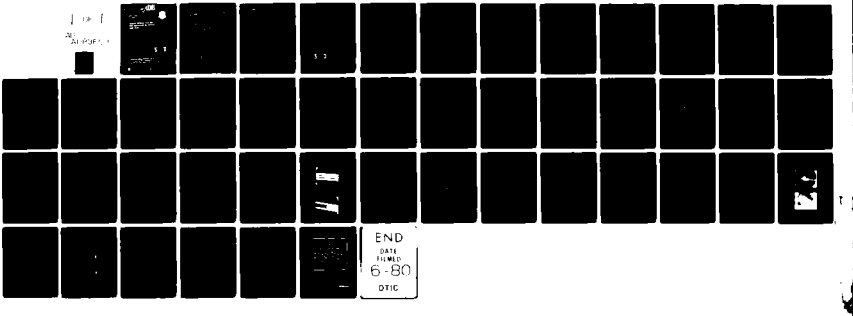

END
DATE FILMED
6-80
DTIC

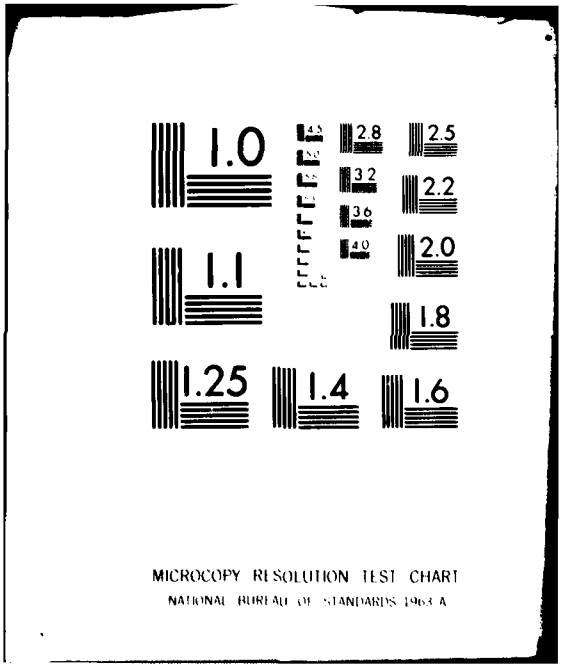
1.0
1.1
1.25
1.4
1.6
1.8
2.0
2.2
2.5
2.8
3.2
3.6
4.0
MICROCOPY RESOLUTION TEST CHART
NATIONAL BUREAU OF STANDARDS 1963 A

UNCLASSIFIED

SECURITY CLASSIFICATION OF THIS PAGE (When Data Entered)

REPORT DOCUMENTATION PAGE

READ INSTRUCTIONS BEFORE COMPLETING FORM

1. REPORT NUMBER: RADC-TR-79-346	2. GOVT ACCESSION NO.
3. RECIPIENT'S CATALOG NUMBER	
4. TITLE (and Subtitle): REMOTE OPTICAL CONTROL AND SWITCHING IN OPTICAL FIBER LINKS	5. TYPE OF REPORT & PERIOD COVERED: Final Technical Report 1 Oct 77 - 30 Sep 78
6. PERFORMING ORG. REPORT NUMBER: N/A	
7. AUTHOR(s): R.V. Gauthier, A.V. Nurmikko	8. CONTRACT OR GRANT NUMBER(s): F19628-78-C-0009 new
9. PERFORMING ORGANIZATION NAME AND ADDRESS: Brown University, Division of Engineering, Providence RI 02912	10. PROGRAM ELEMENT, PROJECT, TASK AREA & WORK UNIT NUMBERS: 61101F, 01767821
11. CONTROLLING OFFICE NAME AND ADDRESS: Deputy for Electronic Technology (RADC/ESO), Hanscom AFB MA 01731	12. REPORT DATE: January 1980
	13. NUMBER OF PAGES: 42
14. MONITORING AGENCY NAME & ADDRESS (if different from Controlling Office): Same	15. SECURITY CLASS. (of this report): UNCLASSIFIED
	15a. DECLASSIFICATION/DOWNGRADING SCHEDULE: N/A

16. DISTRIBUTION STATEMENT (of this Report)

Approved for public release; distribution unlimited

17. DISTRIBUTION STATEMENT (of the abstract entered in Block 20, if different from Report)

Same

18. SUPPLEMENTARY NOTES

RADC Project Engineer: Bernard Bendow (ESO)

This effort was funded in whole by the RADC Laboratory Directors' Fund 01767821.

19. KEY WORDS (Continue on reverse side if necessary and identify by block number)

Optical Switching
Optical Channel Waveguides
Wide Bandwidth Electro-optic Modulation

20. ABSTRACT (Continue on reverse side if necessary and identify by block number)

In this project work, means were considered to achieve high-speed (GHz) switching and modulation in integrated optical circuits, suitable for fiber optics applications. In particular, design and performance criteria were calculated for a planar coupled optical channel device, electro-optically switched by synchronous electrical signals propagating along an asymmetric coplanar waveguide stripline. Design was also executed for several of the components in the laboratory although full integration was not completed within the project period.

DD FORM 1 JAN 73 1473 EDITION OF 1 NOV 65 IS OBSOLETE

UNCLASSIFIED

SECURITY CLASSIFICATION OF THIS PAGE (When Data Entered)

065310

TABLE OF CONTENTS

EVALUATION

This work has potential impact on RADC programs in guided wave optical communications for C^3. The switch design allows rapid optical switching in the GHz regime, an important function for enhancing fiber optics technology.

BERNARD BENDOW
Project Engineer

I. INTRODUCTION

The anticipated needs of future lightwave communications systems have already motivated much developmental activity in integrated optical modulators and switches. In addition to fast data processing applications,such as time-domain multiplexing, a high speed, low drive power modulator offers an alternative to direct modulation of the light source. This allows more freedom in the choice of a light source, and relieves the constraints on analog modulation caused by the highly nonlinear pumping characteristics of semiconductor injection lasers. Therefore, high speed, low drive power light modulators and switches are of considerable importance to the future of optical communications.

In general terms, optical modulators and switches are devices that impress information on an optical frequency carrier by imposing a time-varying alteration of some detectable property of the wave. The information content is proportional to the bandwidth of the imposed variation. The most common nonabsorptive mechanisms for switching and modulation are the electrooptic, magnetooptic and acoustooptic effects. Each can be electrically induced; however, their relative weakness requires relatively large electric, magnetic, or acoustic fields. In bulk devices, these fields of necessity occupy a relatively large volume. Therefore, the stored field energy is high, and the drive power is high in proportion. One of the principle advantages of an optical waveguide modulator over a bulk optical modulator is the substantial reduction of the volume factor allowed by the confinement of the optical beam to a small cross-section over an extended length.

Of the available physical mechanisms for optical modulation and switching, the electrooptic effect has found the most widespread application for a variety of reasons. The devices considered in this work also operate via an electrooptic interaction, specifically, the change induced by an electric field in the index of refraction. We limit our consideration here to a linear

dependence of the index change on the applied field, i.e. the Pockel's effect.

The linear electrooptic effect in a crystalline material can be described by small changes in the size and orientation of the index ellipsoid caused by the applied field. Although the variation of the index ellipsoid is related to the applied field through a tensor which reflects particular crystalline symmetry, a simplified relationship may be found that is useful in estimating the strength of the linear electrooptic effect. For plane polarized light propagating perpendicular to a principal plane of the index ellipsoid, the electrooptic refractive index change may be expressed as $\Delta n = -n^3 rE/2$, where n and r are linear combinations of the principal refractive indices and electro-optic coefficients, respectively, and E is the appropriate component of the applied field. The phase shift of a wave of free space wavelength λ_o traveling a distance ℓ associated with a given index of refraction change is $\Delta\phi = 2\pi\ell\Delta n/\lambda_o$. Using values of n and r typical of electrooptic crystals, the $E\cdot\ell$ product necessary for a π phase shift of .6328μ light is about 20,000 volts. From a standpoint of energy efficiency, it is desirable to confine the electric field to as small a cross-sectional volume as possible. Ideally, the electric field would be applied only in the vicinity of the optical beam.

A glance through the literature reveals the constant striving for reduction of the drive/power of modulators and switches. Integrated optical devices achieve this goal by confining the light beam in one or both transverse directions to a dimension on the order of a vacuum wavelength. Microelectronics techniques allow deposition of electrodes to achieve nearly maximal overlap between the optical and applied electric fields. The large electric fields required for a significant electrooptic effect can be maintained across the narrow interaction region by a very modest voltage. Switches requiring only 2 volts to change the transmitting state have been reported.

The performance of modulators is often specified in terms of the electrical drive power P required to produce a given degree of modulation over a bandwidth Δf. The figure of merit is given as $P/\Delta f$. The usefulness of this

construct is illustrated by considering the bandwidth-drive power tradeoff for a specific device configuration. A typical electrooptic lumped element modulator acts as a capacitive load on the driving ciruit. Its capacitance C is related to the electrode length L and the effective dielectric constant of the structure ϵ through $C = \epsilon C_o L$. Here, C_o is the capacitance per unit length when the electrodes are in free space. The bandwidth for such a device is usually limited by the RC charging time rather than optical transit time considerations. For a resistance R in parallel with the modulator, the bandwidth is $\Delta f = (\pi R \epsilon C_o L)^{-1}$. The drive power is $V_o^2/(2RL^2)$ where V_o is the voltage per unit length needed to produce a given degree of modulation. Bandwidth and drive power are simultaneously varied by adjusting the shunt resistance R. However, there is an unavoidable tradeoff between large bandwidth and low drive power. The figure of merit $P/\Delta f$ reflects the intrinsic energy consumption of the modulator, and is useful as a performance standard independent of optimization for high speed or low drive power.

Although steady improvement in the drive power per bandwidth figure of merit has been reported, most integrated optical modulators have been of the lumped-element type. These devices, when tuned by a shunt resistor to match a 50 ohm generator, have bandwidths on the order of 500 MHz. It is apparent that new device designs are needed to bring speeds into the multi-gigahertz range while still maintaining sub-Watt power dissipation. The device configurations proposed to accomplish this and the focus of this report,are the traveling-wave modulators.

Beyond the charging time limitations in a lumped-element modulator, there is a constraint on the bandwidth caused by the finite transit time of the optical signal. One method that can overcome this involves applying the modulating signal in the form of a co-directional traveling wave. In the ideal case the optical and modulating waves are synchronous, and the bandwidth becomes "unlimited" (limited by external constraints or higher frequency dispersion).

In cases where phase matching does not occur, the bandwidth is limited by the rate at which the two waves get out of synchronization. If a given integrated optical modulator could be operated in either a lumped-element or traveling-wave configuration, a comparison of the figures of merit would prove the more efficient device.

As noted above, the band width of a traveling-wave modulator is limited by the phase mismatch between the light and modulating waves. It can easily be shown that the 3dB bandwidth of a co-directional traveling wave device in the absence of complete phase match is $\Delta f \simeq 1.4c/(\pi(\sqrt{\epsilon} - n)L)$, where ϵ is the 'effective' dielectric constant of the electrode structure and n is the optical index of refraction. The drive power of the device is $P = V_o^2/(2Z_oL^2) = V_o^2C_oc\sqrt{\epsilon}/(2L^2)$ where the characteristic impedence of the line Z_o is expressed as $Z_o = (c\sqrt{\epsilon}C_o)^{-1}$. Comparing the $P/\Delta f$ figures for lumped-element and traveling-wave modulators of the same dimensions, the result

$$(P/\Delta f)_{t.w.}/(P/\Delta f)_{lumped} = \left|1 - \frac{n}{\sqrt{\epsilon}}\right| /1.4$$

indicates that for $\left|1 - \frac{n}{\sqrt{\epsilon}}\right| < 1.4$, the traveling wave configuration is more efficient. This condition is met for most electrooptic materials. As will be shown later, the ratio of figures of merit for devices considered in this work is about 1:3 in favor of the traveling-wave configuration.

Of the few reported investigations into traveling-wave integrated optical modulators, to our knowledge each has resulted in a phase modulator. From a viewpoint of future communications applications, these devices are much less useful than intensity modulators and switches. The impetus of this work, then, was to investigate intensity modulators and switches compatible with integrated optical circuits applications. In particular, efforts were centered on high speed, low drive power devices operating via a traveling wave electrooptic interaction.

II. $LiNbO_3$ CHANNEL WAVEGUIDES--SOME CONSIDERATIONS

An attractive approach to fabricating an integrated optical modulator is to form the dielectric waveguides within the surface region of a good electrooptic material. Then, various surface electrode configurations can be employed to provide an efficient interaction between the confined optical and the modulating fields. Lithium Niobate ($LiNbO_3$) is an excellent electrooptic crystal, exhibiting a large electrooptic coefficient and low optical losses. Considerable effort has been expended to develop waveguides in $LiNbO_3$ by in-diffusion, out-diffusion, ion implantation and epitaxial growth techniques. The methods of in-diffusion and out-diffusion have yielded high quality waveguides with relatively "easy" fabrication.

Lithium Niobate belongs to the 3m crystallographic point group and is ferroelectric. The Curie Point is 1150°C, the melting point is 1253°C. The relative dielectric constants are 28 along the c-axis and 44 perpendicular to it; the dielectric constant is nearly frequency-independent in the constant strain case. $LiNbO_3$ is a uniaxial crystal with an ordinary index of refraction $n_o = 2.29$ and an extraordinary index of refraction $n_e = 2.20$ at the vacuum wavelength of .6328 μm and at room temperature. The crystal is transparent to light of wavelengths from .4 μm to 3 μm. The strongest electrooptic effect occurs when the modulating electric field is aligned parallel to the crystalline c-axis and the light propagates perpendicular to the c-axis. Also, an electric field applied parallel to the crystalline c-axis causes a change in the magnitude but not the orientation of the index ellipsoid. Hence, there is only an index change.

The most prevalent contemporary technique for producing channel optical waveguides in $LiNbO_3$ is an in-diffusion process in which any one of a variety of metals may be deposited on the surface of the crystal and thermally in-diffused to cause a local increase in the index of refraction. The prevalent diffusants are transition metals and their oxides, particularly Titanium (Ti).

Well known deposition techniques allow precise control of the metal film thickness before diffusion and complex waveguide configurations are fabricated easily by the selective diffusion of the photolithographically patterned film. Titanium has a short diffusion length, but the refractive index increase is relatively large. This is advantageous in that the optical waveguide modes are well guided, allowing sharper directional change at guide bends and less loss. In addition, the optical energy is confined close to the crystal surface for efficient electrooptic interaction with surface electrodes. The small guide dimensions (about 3 μm for a single mode), however, make photolithographic patterning non-trivial, particularly for larger devices.

An obstacle to waveguide formation in $LiNbO_3$ by metal in-diffusion is that at the high diffusion temperatures (900 - 1000°C), the substrate loses loosely bound Li_2O through a surface out-diffusion process. This deviation from stoichiometry at the crystal surface increases the extraordinary index of refraction. As a result, a planar waveguide due to Li_2O out-diffusion is formed in addition to the waveguide produced by the metal in-diffusion. In a channel waveguide device, the existance of the background out-diffused planar guide introduces a leak to the channel-guided energy and cross talk between adjacent channels.

$LiNbO_3$ can crystallize in slightly non-stoichiometric form, $(Li_2O)_\nu(Nb_2O_5)_{1-\nu}$, where ν can range from 0.48 to 0.50. It is observed that the ordinary refractive index n_o is independent of ν. However, in the allowed range the extraordinary index n_e increases approximately linearly as ν decreases ($dn_e/d\nu = -1.63$). The reduction of the Li_2O concentration at the surface caused by out-diffusion forms a graded-index waveguiding layer. The microscopic origin of this behavior is not presently understood.

Several investigators have reported techniques to overcome the problem of Li_2O out-diffusion during fabrication of Ti in-diffused waveguides. The methods include treatment of the $LiNbO_3$ sample by Li_2O vapor from a Li_2O

source, $LiNbO_3$ powder, or Li_2CO_3 powder at an appropriate point in the Ti in-diffusion process. The effect of these methods is to either provide a high enough surface vapor pressure of Li_2O from an external source to prevent decomposition of the substrate, or to introduce excess Li_2O into the substrate to compensate for Li_2O loss. Each author claims success, however the reproducibility of these techniques is not established.

Prior to the development of the Ti in-diffusion method, controlled Li_2O out-diffusion was a prevalent technique for fabricating planar waveguides in $LiNbO_3$. The dielectric and electrooptic properties of the out-diffused region are identical with those of the bulk crystal. The refractive index change is small, so the high temperatures($\sim$ 1000°C) and long times required to produce an index change comparable to the Ti in-diffusion process are accompanied by long Li_2O vacancy diffusion depths, typically in the hundreds of micrometers. These deep guides are heavily multimode and the optical energy is not tightly confined near the surface as is desirable for an efficient electrooptic interaction. Li_2O out-diffused waveguides were quickly supplanted by the Ti in-diffusion process which gave comparable index changes with guide depths of a few micrometers. In addition, the in-diffusion process is easily amendable to photolithographic patterning of channels, and the ability to control the amount of diffusant adds a critical parameter to tailor the guid index profile.

A novel adeptation of the Li_2O out-diffusion process has been developed by Lee and Goldberg [1] for channel waveguide formation. The technique involves masking out-diffusion with a capping layer. A thin layer of SiO_2 is deposited on the crystal surface and the complement of the waveguide pattern is formed in the SiO_2 film by photolithographic techniques and etching. The out-diffusiton is carried out at the standard temperature ($\sim$ 930°C) but only for a very short time ($\sim$ 25 minutes). The SiO_2 layer caps the Li_2O out-flow, so the index change occurs only at the $LiNbO_3$ surfaces exposed by

the channels in the SiO_2. The short diffusion time allows only a rather small index change, and single mode guides are reported with lateral dimensions up to 15 μm. This five-fold increase in guide width over single mode Ti in-diffused guides significantly eases photolithographic tolerances. As Goldberg and Lee note, unlike the in-diffusion process, where unwanted out-diffusion of Li_2O can also cause an increase in n_e, the use of out-diffusion by itself for waveguide fabrication avoids the problem of having two competing index-increasing processes. Finally, it must be noted that the out-diffused guides do not guide light of the n_o polarization; fortunately this polarization has an electrooptic coeffient only 1/3 the value of the guided n_e polarization.

III. INTENSITY MODULATION AT HIGH FREQUENCIES IN CHNNEL WAVEGUIDES

a. General Background

Basic configurations for contemporary planar channel waveguide modulators, mainly of signle mode type, are shown in figure 1. The first structure, the directional coupler, is characterized by the periodic transfer of power between the two guides as the optical signal propagates along the structure. The principle of the directional coupler is modal interference of the eigenmodes of the two-guide system. The parallel dielectric waveguides interact via their evanescent fields thereby forming a loosely coupled system. The propagation distance required for the maximum optical energy to be transferred from one guide to the other is the coupling length ℓ. Although the physical length of the device is fixed, the coupling length may be varied electrooptically. Kogelnik and Schmidt have, however, taken advantage of a phase reversal technique ("stepped $\Delta\beta$ reversal") which significantly reduces the need for predetermined coupling lengths [2].

The Balanced Bridge (Integrated Mach Zehnder Interferometer), as illustrated in figure 1b, also operated by modal interference. However, the power coupling regions and the electroopically tuned modulation region are separate. The optical carrier entering either input part is split equally by the 3dB coupler into the two branching arms of the interferometer. In the section where the waveguides are spaced far enough to prevent coupling, a relative phase shift in a given channel can be obtained by an electrooptically induced index of refraction change. When the two light beams are recombined at the second 3db coupler, the relative power between the output channels is controlled by the induced phase shift. The types of structures used to produce the 3dB coupling sections include directional couplers, tapered velocity couplers, and branching waveguides.

The transfer characteristics of the directional coupler and the balanced bridge are somewhat different, and have been discussed in some detail in the

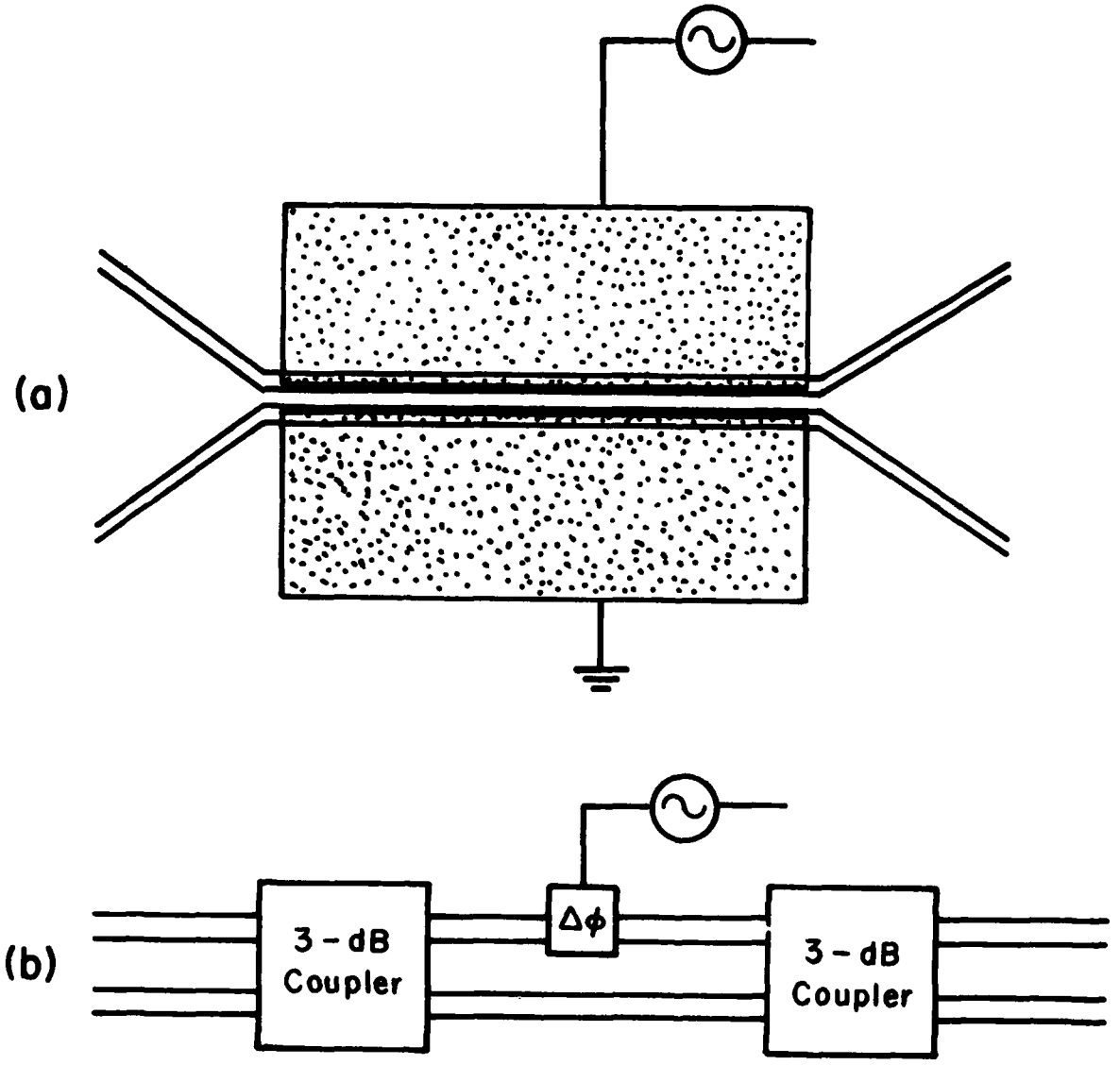

Figure 1

literature [3].

A major advantage of the balanced bridge modulator/switch over the directional coupler in high-speed integrated optical devices is the separation of power coupling and modulation functions. This allows the design for each to be selected and optimized separately. In addition, the modulation element is only required to produce a net terminal phase shift. The directional coupler, on the other hand, is analyzed with the assumption of constant distributed modulation. The integrating effect of the balanced bridge is more adaptable in overcoming losses and fabrication errors. A liability, however, is that the balanced bridge requires series connection of three device sections, resulting in a long device that may increase losses, may require more directional changes in the optical guiding, and one that is harder to fabricate due to complexity and increased electrode contacts.

Integrated electrooptic modulators are naturally compatible with planar electrode structures. On insulating dielectric materials, the fringing fields from electrodes deposited on or near the substrate surface penetrate to a depth comparable to the electrode separation. Optical channel guides in this vicinity provide an efficient interaction volume for light modulation via the electrooptic effect. For use at high frequencies, electrooptic modulators require carefully tailored electrodes to reduce capacitance. However, contemporary microelectronics fabrication techniques, initially for semiconductor device processing, are available for fabricating integrated optical circuits.

For devices in which the modulating fields is applied via a traveling-wave structure, it is desirable to maintain the same compatability with planar device technology. This suggests the investigation of microwave integrated circuits, particularly those planar configurations in which all conductors are located on the same dielectric surface. In addition to being simpler to fabricate, surface strip transmission lines are relatively insensitive to dielectric substrate thickness.

$LiNbO_3$ as a uniaxial crystal has principal relative dielectric constants $\varepsilon_{xx} = \varepsilon_{yy} = 43$ and $\varepsilon_{zz} = 28$, where the z direction is taken along the 'optical' axis. For surface electrode structures, large relative dielectric constants mean efficient use of the modulating voltage: most of the electric field energy resides in the dielectric, where it can interact with the guided optical field. It is easy to show that in cases where the crystal optical axis is perpendicular to the strip electrode axis, the anisotropic dielectric can be replaced with an isotropic dielectric with effective relative dielectric constant $\varepsilon_{eff} = (\varepsilon_{xx}\varepsilon_{zz})^{1/2}$.

One potentially useful surface strip transmission line form is the coplanar waveguide. It consists of a thin conducting strip deposited on the surface of a dielectric slab with two ground electrodes running adjacent and parallel to the strip on the same surface, as illustrated in figure 2a. There is no low frequency cutoff because of the quasi-TEM mode of propagation. The vertical componant of the fringing field in the dielectric reverses direction twice as the structure is traversed, and the horizontal component is oppositely directed in the gaps. Both polarity effects are potentially useful in device applications.

The characteristic impedance Z_o of a coplanar waveguide fabricated on a dielectric half-plane with relative dielectric constant ε_r has been calculated by Wen [4]. He shows that Z_o is a function of the ratio a/b where 2a is the width of the center strip and 2b is the edge-to-edge separation of the ground electrodes. It is assumed that the outer ground electrode edges are far apart ($c = \infty$). Using a zeroth order, quasi-static approximation, conformal mapping yields the capacitance per unit length.

$$C = (\varepsilon_r + 1)\varepsilon_o 2K'(m)/K(m)$$

where K(m) is the complete elliptic integral of the first kind, K' is the complete elliptic integral of the second kind, and the argument m is given by

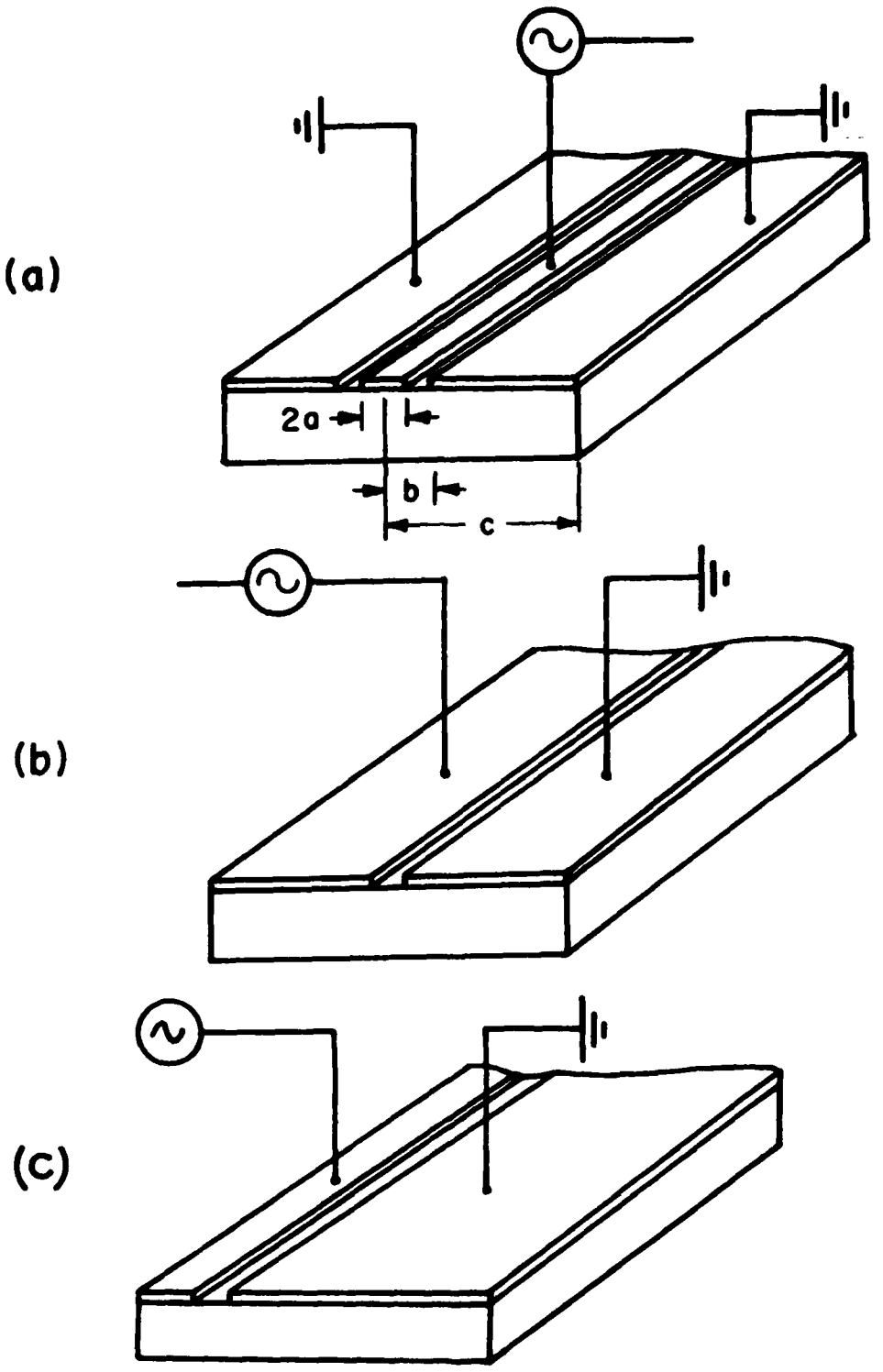

Figure 2

$$m = a/b.$$

Wen accounts for the finite width of the ground electrodes by taking

$$m^2 = (a/b)^2[1 - (\omega/c)^2]/[1 - (a/c)^2]$$

For a thin planar electrode structure on the interface of air and dielectric half planes, the transmission line is treated as being totally immersed in a dielectric of effective dielectric constant $(\epsilon_r + 1)/2$. The phase velocity for propagation of a TEM mode through such a medium is

$$V = C/\sqrt{(\epsilon_r + 1)/2}$$

$$= C/[(\sqrt{\epsilon_{xx}\epsilon_{zz}} + 1)/2]^{1/2} \text{ for } LiNbO_3.$$

For a $LiNbO_3$ substrate, the ratio of C/β ("refractive index") for the traveling modulation wave is 4.2. The characteristic impedence of the coplanar waveguide is given by

$$Z_o = \frac{1}{Cv} = \frac{1}{2\sqrt{2}c\epsilon_o(\epsilon_r + 1)^{1/2}} \frac{K(m)}{K'(m)}$$

Some analysis of the coplanar waveguide has extended the treatment beyond the idealized structure. Cases in which the electrode thickness is not insignificant compared to the gap width and cases where the substrate thickness is not very much greater than the gap width have been investigated. These studies, however, are largely theoretical rather than design oriented. They do serve to point out where the simple model weakens and second order effects must be taken into account. Also, experimental verification of the quasi-static approximation analysis shows some conflict.

Another potentially useful surface strip transmission line is the dual of the coplanar waveguide, the parallel strip coplanar line (PSCL), shown in figure 2b. The two strip electrodes are identical; either can be grounded and the other conducting. The horizontal component of the electric field is unidirectional in the gap, but the vertical componant reverses sign between strips. This feature can be exploited to increase the efficiency of an

electrooptic interaction.

Again, since the field lines between the conducting and ground strips are not confined entirely to the substrate, the propagating mode along the line is not purely transverse (TEM), but quasi-TEM. There is no low frequency cutoff. However, at high frequencies, the ratio of longitudinal to transverse electric field becomes significant and the propagating mode may no longer be treated as quasi-TEM. Analysis of this "hybrid mode" is far more rigorous. The approximation has been shown by experiment to be fairly good up to X-band frequencies.

The capacitance per unit length of the PSCL is found by a conformal mapping to be

$$C = (\varepsilon_r + 1)\varepsilon_o \frac{2K(m)}{K'(m)}$$

with $m = a/b$, where 2a is the gap width and 2b is the separation of the outer edges of the electrodes. The phase velocity is the same as that of the coplanar waveguide, so the characteristic impedence is

$$Z_o = \frac{1}{2\sqrt{2}C\varepsilon_o(\varepsilon_r + 1)^{1/2}} \frac{K'(m)}{K(m)}$$

It is noteworthy from the point of view of fabrication tolerances to observe that the characteristic impedance does not depend strongly on the ratio of the electrode strip width to gap ratio. For a nominally 50 Ω line on $LiNbO_3$, the strip width to gap ratio may vary from 1.2 to 2.0 while Z_o remains within 50 ± 2 Ω. Therefore, the PSCL can be fairly easily matched to the generator impedance.

The PSCL has been tested experimentally by Izutsu et. al. in a phase modulation configuration [5]. The results support the analysis of the line characteristics, however several resonances due to input and output discontinuities marred operation at frequencies above 3 Ghz. A novel variant of the

PSCL was proposed and tested by Izutsu et. al. that showed improved frequency response of the modulation characteristics. The asymmetric PSCL is illustrated in figure 2c. The analysis of this novel arrangement has been considered by us by using a conformal mapping technique. In addition, we have assumed that the 50 Ω line on $LiNbO_3$ should be scalable as long as the aspect ratio (a/b) is fixed.

b) Focus of This Research

The present investigation of high-speed integrated optical intensity modulators and switches has resulted in a number of proposed device designs. All devices are based on a traveling wave electrooptic interaction. However, the designs are naturally grouped according to optical waveguide fabrication technique and modulation configuration. A prototypical design from each group will be discussed after a few common considerations are introduced.

Of the few schemes proposed for phase-matched electro-optic interaction in $LiNbO_3$, none are amenable to an integrated optical format. In the absence of phase matching, the modulation bandwidth of a traveling wave device is inversely proportional to the interaction length

$$\Delta f = 1.4\ c/r(\sqrt{\epsilon_r} - n)L$$

As calculated earlier the drive power is proportional to L^{-2}

$$P = V_o^2\ c\sqrt{\epsilon_r}\ C_o/(2L^2)$$

Thus the figure of merit, $P/\Delta f$, is always improved by lengthening the interaction region at the expense of bandwidth. For this reason, effort has been made to keep the bandwidth above 3 GHz while the 100% modulation voltage is assumed to be held at about 7 volts or less. This assures that these results are not only novel, but potentially useful: the bandwidth and drive power are compatable with the emerging high-speed GaAs FET technology.

All devices proposed here are planned for a Z-cut $LiNbO_3$ substrate. This is because initial work anticipated employing the unique electric field distribution provided by the coplanar waveguide in the cobra configuration. Since all designs were made with fabrication as the ultimate goal, the initial purchase of Z-cut substrates was a constraint.

Channel waveguides in Z-cut $LiNbO_3$ can guide two families of normal modes according to the analysis of Marcatili [6]. The small axial field components

make the light waves essentially TEM in character, with one family of modes polarized perpendicular to the substrate surface and one family polarized parallel. Perpendicular polarization gives rise to extraordinary waves that respond to the r_{33} electrooptic coefficient for a z directed modulating field. Guided light polarized parallel to the surface is an ordinary wave connected with the electrooptic coefficient r_{13}. Since r_{33} has a value three times that of r_{13}, it is much more efficient to modulate the extraordinary wave. This is fortuitous for out-diffused waveguide, as the extraordinary wave is the only one that can be guided. For Ti-indiffused waveguides, however, this is a problem; to guide the extraordinary wave, the Li_2O out-diffusion must be stopped or compensated

In a "Cobra" electrode configuration, the metallization is deposted right above the optical guiding channel, (see figure 3). This can represent a significant source of loss for the perpendicular polarization. The reason is that the boundary condition for a normal electric field allows substantially more penetration into a non-perfect conductor than for the tangential component. Thus, the mode with normal electric field will show more loss due to the presence of the metal boundary. Kaminow and Stulz [7] suggest isolating metal electrodes from the dielectric waveguide by a thin dielectric buffer layer. The buffer layer should have as low a refractive index as possible to assure rapid decay of evanescent light field, and it should have as high a dielectric constant as possible to minimize voltage drop across the buffer layer. Likely materials include Al_2O_3 and SiO_2. Kaminow and Stulz report reduced losses with a 2000A thick layer of Al_2O_3 on $LiNbO_3$. Care must be taken, however, since the recent analyses of this multilayer structure show that instead of decreasing monotonically with increasing buffer thickness, the optical attenuation actually peaks at non-zero buffer thickness.

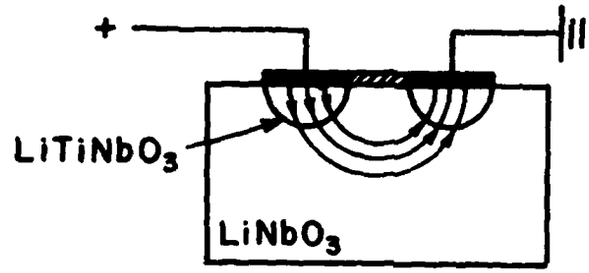

FIGURE 3

Directional Coupler with Ti in-diffused Guides

The directional coupler using stepped $\Delta\beta$ reversal, as proposed by Kogelnik and Schmidt [2], can be achieved in an electrooptic device by reversing the polarity of the applied electric field in each successive step. A 6-section device, for example, uses 3 Cobra electrodes meandering back and forth above the optical channels. The applied field (and consequently the phase mismatch $\Delta\beta$) reverses 5 times along the structure when the center electrode is grounded and a single drive voltage is applied to the outer electrodes. In case of the 6 sections, the unused electrode is spaced far from the other two.

Such a device could be adapted to a traveling-wave configuration by replacing the lumped element electrodes with a zig-zagging coplanar waveguide. The electric field distribution under the coplanar waveguide has a normal componant that changes polarity between the ground electrodes and the conducting strip. The Cobra configuration applies a strong normal field in the optical channel region, and in a manner identical to that of Schmidt and Cross [8] (by shifting the center conductor above alternate channels in successive sections) the alternating polarity of $\Delta\beta$ can be achieved.

It is assumed here that the reported optical properties of the Schmidt and Cross device are accurate and reproducible, and that by following their procedure, similar guides could be fabricated. They have produced two 3 μm wide singlemode optical channel waveguides by Ti in-diffusion into Z-cut $LiNbO_3$ using well documented techniques. In the optical coupling region, the waveguides are spaced 3 μm edge to edge over a length of 10.5 mm, which they found to be 5.8 coupling lenghts. As noted earlier, the most efficient switching will occur in a device sectioned in the integer closest to its interaction length in units of coupling length. Here, 6 sections are called for.

An upper bound for the required switching voltage, assuming a device biased into one state, can be estimated from the switching characteristics of the $\Delta\beta$ couplers. It follows that the required phase mismatch is bounded by

$$\Delta\beta L \gtrsim 2\pi$$

So for $\Delta\beta = \frac{2\pi}{\lambda}\Delta n$ between guides, the index change required for each guide is

$$\Delta n \gtrsim \lambda/21$$

The electrooptically reduced index change in $LiNbO_3$ from a z directed electric field is

$$\Delta n = n^3 r\, E_z/z$$

The electric field fringing in Cobra configuration may be estimated from an expression derived by Marcuse

$$E_z = 2V/(\sqrt{2}\pi g),$$

where g is the gap spacing between electrodes. Thus, the switching voltage is bounded by

$$V \gtrsim \frac{\sqrt{2}\pi\lambda g}{2n^3 rL}$$

To limit current through the coplanar waveguide, it is desirable that the characteristic impedance be at least 50 Ω; the 50 Ω value is particularly convenient since it matches most sources and test equipment. It can be shown, using the inversion formulae for elliptic integrals, that the required aspect ratio (a/b as defined in figure 2a) assuming a very large c, is

$$a/b = .118$$

For a 3 μm electrode gap (b - a = 3 μm) to match the channel waveguide separation, the width of the central conducting electrode is approximately .8 μm (a = .4 μm). Calculations support the anticipation that electrodes narrower than 10 μm become excessively lossy. Therefore, a coplanar waveguide with 50 Ω characteristic impedence seems unrealizable for these dimensions.

However, by allowing a 15 μm wide center conductor and 3 μm gaps, the characteristic impedence of the line is only reduced to 25 Ω, which may be acceptable for some applications.

Resistive loss in the conductors is expected to be a significant problem for this modulator configuration. Since the analysis is made assuming constant magnitude of $\Delta\beta$ throughout the device, attenuated voltage would reduce the electrooptic effect so the phase correlation decayed in each section and from section to section. Perhaps this could be compensated by adjusting the electrode length or placement; however, the effect would have to be well-characterized in advance.

Another potentially deleterious effect is the result of the zigzagging coplanar waveguide. It is expecced that this will give rise to radiation and frequency dependent reflection. The zig-zag transition must be made fairly abruptly so that the cascaded $\Delta\beta$ sections appear contiguous. Perhaps coherent radiation effects could be avoided with unequal step lengths.

The difficulties notwithstanding, the use of a coplanar waveguide provides a novel and useful way of introducing traveling wave interaction to the stepped $\Delta\beta$ directional coupler. In particular, the designs considered in this project work were directed toward the development of coplanar guides up to frequencies of 10 GHz.

Balanced Bridge with Ti In-diffused Guides

The balanced bridge configuration, which was analyzed by Ramaswamy and Standley [3] for use as an integrated optical switch, appears well suited for traveling-wave operations. The lumped-element electrodes in the phase shifter may be replaced by a microwave integrated transmission line. The advantage of the balanced bridge over the directional coupler is that the coupling and modulation functions may be separately optimized. Also, the modulation transfer function depends only on the integral of the distributed phase shift. The effect of inevitable fabrication errors and conductor losses may be compensated for by a d. c. bias voltage.

The balanced bridge incorporates a parallel strip coplanar waveguide (PSCW) in the modulation section; the 3dB coupling may be provided by dc biased directional couplers. The use of directional couplers is preferred over "y" branching waveguides because the optical beam is always guided in the directional couplers and their directionality is better suited to switching operations. The PSCS is aligned in the Cobra configuration over one branch arm and a lumped electrode biasing set covers the other arm. It is expected that symmetry between the branch arms is critical to achieving low cross-talk. Thus, unlike the device proposed earlier by Ramaswamy and Standley, the arms branch in a symmetric geometry and the position and area covered by the metallization is made as similar as possible.

The PSCW used in the modulating section is designed for a 50 Ω characteristic impedance. The aspect ratio is W/g = 1.6, so the electrodes are each 16 μm wide, and are separated by a 10 μm gap. The PSCW can modulate only one arm or it can be used in a "push-pull" configuration where a Cobra electrode covers each branch arm and induces opposite pulse shifts in each. For identifical PSCW's, the push-pull" modulation is twice as efficient. However, that con-

figuration requires that the PSCW gap width equals the branch arm separation. If wide branch arm separation is necessary, for example, to achieve good channel isolation, single arm modulation may be more efficient: halving the PSCW gap doubles the electric field under either Cobra electrode. Of course, the strip width is halved also to maintain a constant aspect ratio, so that care must be taken to prevent conductive losses from becoming excessive. Our early designs made use of single arm modulation because the channels were separated for good isolation and because it was thought desirable to keep the microwave line as far from the dc electrodes as possible to avoid ac coupling. After the PSCW leaves the interaction region, it can be either terminated in a matched resistance or coupled back off the substrate.

The z directed electric field under the Cobra electrodes of the PSCW is given by

$$E = \frac{2V}{\sqrt{2}\eta g}$$

and the phase change in the branch arm due to the applied modulation voltage is

$$\Delta\phi = \frac{2\eta}{\lambda}\Delta nL = \frac{2n^3 rVL.}{\lambda\sqrt{2}g}$$

The figure of merit is halved for the case where "push-pull" modulations is used. A device assuming lossless 16 μm conducting strips with a 10 μm gap and an interaction length of 8 mm, has a calculated switching voltage of 7V.

The many advantages of the Ti and indiffusion process have made it the most widely used technique for channel waveguide fabrication in $LiNbO_3$. The deposited metal film may be photolithographically patterned and selectively diffused into the substrate; the resultant channel waveguides are low loss tightly

confining. The small cross section guides keep the optical signal close to the substrate surface, and the relatively large index difference allows for fairly strong directional changes. Using the published results of work at Bell Laboratories as a benchmark, single mode channels for .6328 μm light may be produced by in-diffusing 3 μm wide Ti strips. Of course, uniform guides require that the pre-diffused strips be without variation or flow along the entire length of the channel, typically the length of the device (10 - 25 mm). The techniques for such ultrafine fabrication are a science in themselves, and the equipment and technology are presently available in but a handful of laboratories.

In attempting to circumvent the constraints of available funds and equipment, alternative waveguide fabrication techniques were reviewed by us. The capped out-diffusion method of Goldberg and Lee is well suited to the available facilities at Brown University. They have reported single mode channel waveguides for .6328 μm light having channel widths of $\sim$ 15 μm. The channels are defined by etching openings in the capping SiO_2 glass layer, and patterns of such dimensions are within the range of Brown University's facilities. Therefore, device designs have been pursued based on the modal properties of Li_2O out-diffused channel waveguides.

The cause of the large channel cross section, even for a single mode guide, is that the out-diffusion process results in a very small change in the extraordinary refractice index of $LiNbO_3$. The light is only weakly guided; as can be seen from a simple critical angle argument, even a small angle bend will cause the guided beam to radiate into the substrate. Therefore, it is not expected that bends and curved sections may be used to accomplish directional changes in a device with out-diffused waveguides. It would be advantageous to use straight line guides that do not bend at all. For this reason, a three guide coupler has been investigated.

The three guide coupler is a generalization of the two guide directional coupler which has already been discussed. As illustrated in figure 4 , the three guide coupler consists of three parallel coplanar guides spaced closely enough that the evanescent fields of adjacent guides cause weak coupling. This structure has so far received far less attention than the directional coupler, however, its unique properties make it attractive as an effective integrated optical beam splitter without bends.

An analytic treatment of the modes of a three guide structure has been published by Iwasaki et.al.[9]. For the case of identical guides spaced by equal separations, there exists a length ℓ' after which all optical power initially in the central guide will be split evenly between the outer guides. After propagating another length ℓ', the power in the outer guides has returned to the central guide. This suggests beam splitting and recombination operations. A three guide coupler section of length ℓ' may have only the center input channel excited, and at the output, the power is evenly divided between the outer guides, with no power in the central guide. If the central guide is terminated at the end of the ℓ' length section but the outer guides continued, their interaction is negligible with the result that the single input beam has been equally divided into two isolated output channels. The lateral power flow is accomplished not by angle bends in a single guide, but by modal interference in a multiple straight guide section. For recombination, the treatment of Iwasaki et.al. shows that for equal intensity in-phase signals entering the outer guides of an ℓ' length section, all optical power at the termination will reside in the central guide. However, for components of equal intensity but π out of phase entering the outer channels, the light exiting a section of length ℓ' is entirely in the outer guides. Termination of the outer guides of such a section causes the structure to respond to a 0 or π phase in the

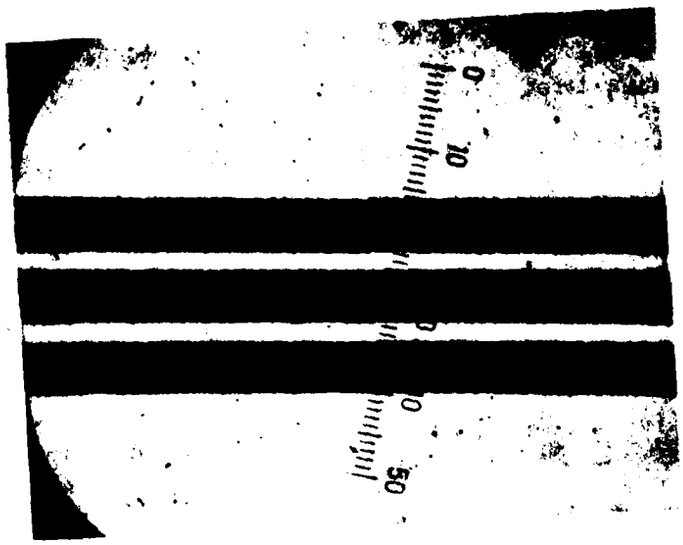

FIGURE 4

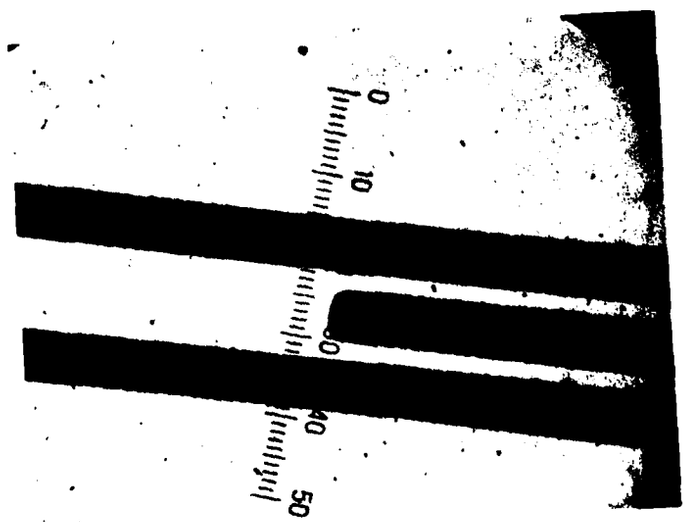

separated inputs by either exiting all power out the central guide or scattering all light at the 'dead' ends of the outer guides.

By using out-diffusion as the optical waveguide fabrication technique and two three-guide couplers for power splitting and recombination, a balanced bridge switch has been designed for fabrication at Brown University's facilities. As illustrated in figure 5, the input channel leads to the central part of the three guide coupler. The central guide of the coupler is terminated after one lateral coupling length ℓ', and the outer guides continue to form the non-interacting branch arms of the balanced bridge switch. The recombination coupler, again of length ℓ', is fed by the branch arms. The outer channels terminate at the end of the coupler section, with only the central channel continuing on as the output part of the device. An asymmetric PSCL applies the traveling-wave modulating field in an efficient push-pull configuration through the Cobra electrodes. The optical channel wave guides are 15 μm wide, and in the three guide coupler sections, the guide edge-to-edge separation is 6 μm. The 50 Ω characteristic impedence microwave line has a 16 μm wide conducting strip separated from the ground plane by a 27 μm gap. At both ends, the PSCL dimensions are expanded into contact pads; however, the aspect ratio is kept constant to avoid changes in the characteristic impedence.

The voltage to induce a π phase shift between the branch arms is

$$V_\pi = \pi\lambda\sqrt{2}g/4n^3rL$$

where L is the interaction length and a push-pull configuration is assumed.

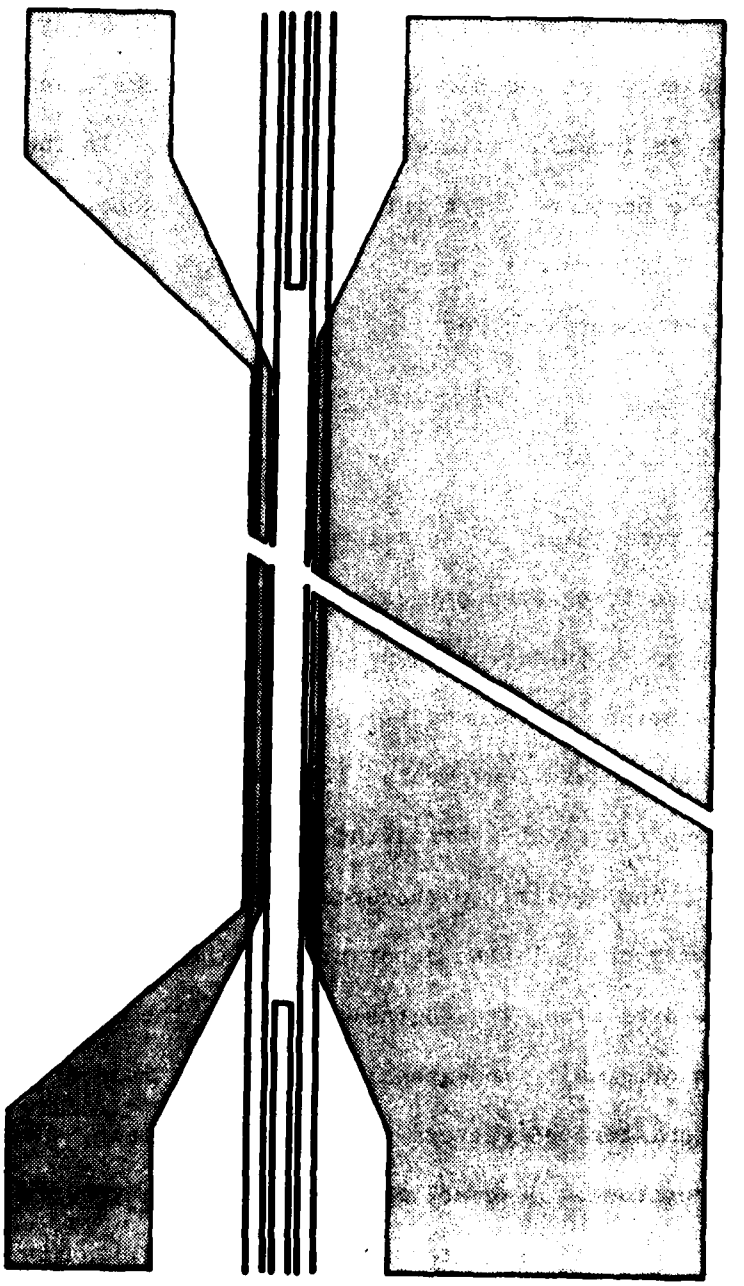

Figure 5

Thus, assuming that the bandwidth Δf is limited by phase mismatch, the figure of merit for this device is

$$P/\Delta f \approx 1.9 \lambda^2 g^2(\sqrt{\epsilon} - n)/(cr^2L^3n^6Z_o)$$

The balanced bridge switch with out-diffused waveguides is not a very satisfactory switch because in the off-state, the light signal is scattered indiscriminately out the back of the device rather than remaining guided but having its location altered to another part. In the off-state, some light will be scattered back into the output channel, degrading the on-off contrast. This compromise must be made, however, when constrained to work with straight-section guides.

Experimental Evaluation

The initial intent of this investigation was to design and fabricate traveling-wave integrated optical modulators based on the well-studied and documented Ti in-diffusion process for channel waveguides developed at Bell Laboratories. Such processing, however, requires sophisticated techniques and often ultramodern equipment. After much time and effort were invested, it became apparent that fabricating such devices at Brown University was not possible due to limited resources.

A first problem is the generation of the photo mask. The aspect ratio (3 μm linewidths along 1" lengths) precludes the use of rubylith in making the pattern original. An extensive search was made of facilities operating the more sophisticated pattern generating equipment, such as the David Mann pattern generators. However, the cost of such a service proved to be prohibitive. In addition, tests by us using small patterns with 3 μm linewidths resulted in generally poor photolithographic transfer. The lack of a well collimated light source, a proper mask-substrate aligner and adequate clean-room facilities contributed to the impracticality of 3 μm photolithography.

When it became apparent that single mode optical waveguides produced by the Ti in-diffusion method were unlikely to succeed, attention was focused on the Li_2O out-diffusion method. The first experiment was designed to produce a planar optical waveguide in Z-cut $LiNbO_3$ by out-diffusion of Li_2O. The 8 mm, x 6 mm $LiNbO_3$ samples were cleaned by the standard processes, and then sealed in clean quartz ampules which were evacuated and backfilled with 50 microns of oxygen. After baking in a 980°C furnace for the prescribed out-diffusion time, a given quartz ampule was broken open to readmit atmospheric air and the sample was reoxidized at the out-diffusion temperature (980°C) for 5 minutes. Three tests were conducted, with diffusion times of 25 minutes, 40 minutes and 2 hours.

To determine the presence of a guided mode or modes in each of the three cases, the following test setup was used. A HeNe laser operating at .6328 μm was aligned parallel to the polished crystal surface and focused with a 20x microscope objective on the crystal edge. It was usually apparent that much of the incident light was being scattered, and thus the small guiding effects were difficult to observe. Therefore, the incident beam was polarized at 45° to the crystal z axis and passed through a polarizer that could be rotated from 0° to 90° from the crystal z axis. The intensity incident on the crystal is the same in both situations, and thus the scatter remained approximately unchanged. However, with the adjustable polarizer parallel to the crystal z axis, bright beads of light could be observed along the exit edges of the guides. This effect disappeared when the polarizer was rotated to perpendicular to the crystal z axis, which was expected because Li_2O out-diffusion does not affect the ordinary refractive index.

A second experiment was performed to verify optical guiding in out-diffused channels. For this purpose, a photomask for a 15 μm wide channel of 8 mm length was produced using a two-step reduction from a 50 x rubylith

original. Meanwhile, an approximately 2000 Å thick SiO_2 film was electron beam evaporated onto the clean polished faces of 8 mm x 6 mm x 1 mm z-cut $LiNbO_3$ substrates. The film thickness was estimated by the reflected color, but the thickness is not critical since the layer serves only to cap Li_2O out-diffusion. Hunt 104 positive photoresist was spun on the substrate, exposed through the photomask, and developed. The channel in the developed photoresist was visible with a microscope. It served as the masking template for etching the channel into the capping SiO_2 layer with buffered HF. After this step, the photoresist was stripped and the substrate sealed in a quartz ampule which had been evacuated and back filled to 50 microns of oxygen. The diffusion step consisted of a 25 minute bake in a 930°C furnace followed by a 5 minute reoxidation bake in atmospheric air at 930°C.

With a setup similar to that used to test the thin film guides, the presence of a guided mode was clearly observable in these channel waveguides. The substrate was carefully aligned so that the light beam was focused on the crystal edge at the channel end and was directed along the channel axis. In addition, both crystal end faces were polished. Again, in both polarization states, most incident light went to background scatter. However, the bright pinpoint of light visible at the channel termination was present only for the extraordinary wave.

After these preliminary tests to prove the feasibility of channel guiding in Li_2O out-diffused guides, a balanced bridge traveling-wave modulator was designed and its fabrication attempted. The photomask for the optical waveguides was proportioned according to calculations.The firm of Precision Art Coordinators of Providence, RI, produced the photomask by mechanically cutting the original in rubylith at 50 x and photoreducing in a single step. Of the 20 masks delivered, 6 were deemed dimensionally correct and of sufficient quality to be usable. The photomasks for the optical channels were clear field, implying the need for

negative photoresisting. The photomask for the asymmetric PSCL was fabricated at Brown University at 50 x in rubylith and photographically reduced in two steps. This mask was clear field, since it was felt that this would aid in the registration of the mask over the optical waveguide pattern. The need for visual alignment of the electrode structure over the optical waveguide pattern unfortunately precluded the use of an etch technique for electrode fabrication. Instead, a liftoff technique was used.

A typical fabrication run proceeded as follows. The 25 mm (x) x 10 mm (y) x 1 mm (z) $LiNbO_3$ substrate was carefully cleaned according to the standard cleaning process in semiconductor industry. A 800 Å to 1200 Å SiO_2 film was then electron beam evaporated onto the polished z-cut $LiNbO_3$ face. The approximate thickness was checked by the reflected color test, and pin holes, large particles and poor adhesion were cause for rejection at this stage. The Kodak 747 negative photoresist was then spun on and prebaked. Rejection at this point was most often caused by macroscopic particles incorporated in the resist. The optical waveguide photomask was aligned over the substrate and the resist exposed, developed and postbaked. The desired close contact of the mask to the resist often resulted in adhesion of some resist to the mask. Since this could not be cleaned without destroying the emulsion mask, masks were only useful for a couple exposures. Uneven mask-substrate contact was a severe problem, and its effects could be seen in shallow channels, bridging, poorly defined channel edges and incorrect dimensions. The developed resist was used as a masking template for the buffered HF etch of the waveguide pattern into the SiO_2 film. At this point, rejection could be caused by poor photoresist adhesion, where the SiO_2 would quickly over-etch.

The next step was to evacuate, back fill to 50 microns of oxygen and seal the sample in a double quartz ampule. This arrangement uses the inner quartz tube as a baffle to protect the sample from quartz shards which implode when the scaled outer tube is broken open. The quartz chips and dust would be bonded to the substrate during the subsequent high temperature reoxidation bake and ruin the surface flatness. Although the heat treatment had produced no cracked samples during the preliminary tests using the smaller substrates, the first two device-sized substrates were cracked during diffusion. This situation was remedied by supporting the sample on a clean alumina flat within the inner quartz tube.

After the out-diffusion step, a thin ($\sim$ 600Å) layer of SiO_2 was electron beam evaporated onto the substrate surface. The previous SiO_2 layer could not be removed, since the reflected color differences caused by the channels in the SiO_2 were the only means of locating the optical channels. The purpose of the second SiO_2 layer was to act as a low refractive index buffer region between the optical guide and the electrode metallization. Of 16 attempts, only one device (#15) was brought successfully to this stage of processing. Figure 6 shows color photographs of device #15 after the SiO_2 buffer layer was deposited. The thicker capping SiO_2, which had undergone the thermal stresses of the out-diffusion temperature plus the etching effects of Li_2O vapor, appears as the mottled blue area. The optical channels are under the brown-orange thin SiO_2 buffer.

In parallel with the effort to produce the balanced bridge channel waveguides in $LiNbO_3$, fabrication of the asymmetric PSCL electrodes by lift-off was attempted. For practice, a thin SiO_2 film was deposited on a clean polished $LiNbO_3$ surface and the electrode configuration photolithographically patterned in negative resist. The developed resist remained in the complement of the desired electrode pattern. A thin aluminum film was then deposited over the entire substrate surface and the remaining photoresist stripped.

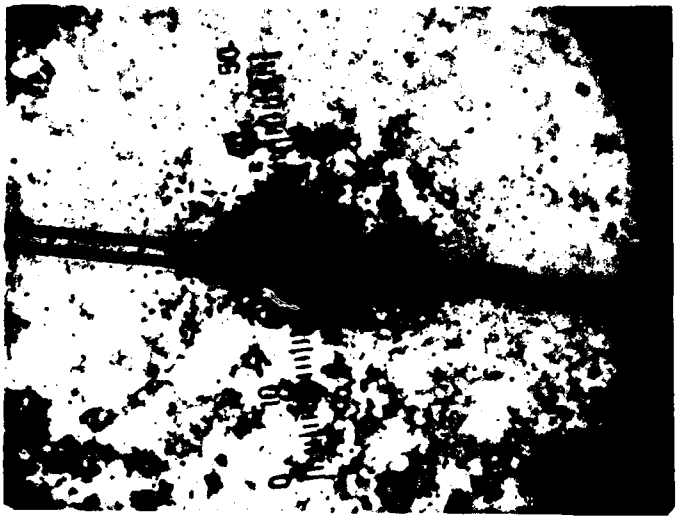

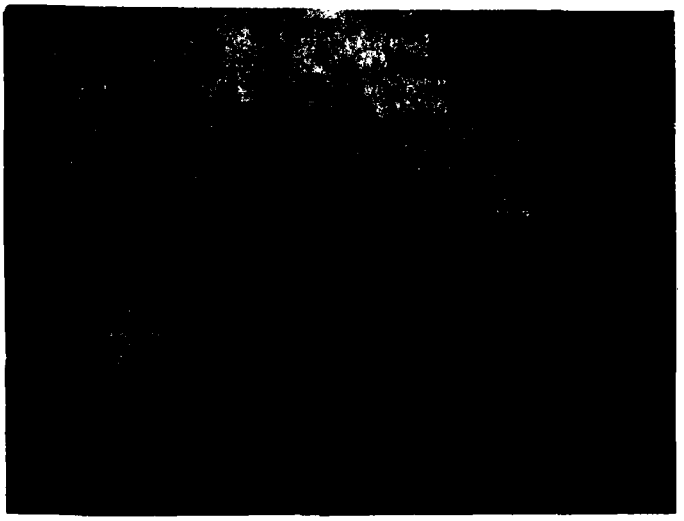

Figure 6

In every trial case, the entire aluminum layer lifted off during the strip stage, indicating poor adhesion of the aluminum to the uncovered substrate surface. Also, inadequate thickness monitoring equipment resulted in many films which were too thick and pealed off in a foil.

Despite the lack of previous success, an attempt was made to fabricate the asymmetric PSCL structure on device #15 with the lift-off technique. The negative resist was spun on and pre-baked, the electrode photomask carefully aligned, and the photoresist exposed, developed and post-baked. Figure 7 shows pictures of the developed photoresist with the electrode pattern carefully aligned over the branch arms of the optical channel pattern. Following the deposition of a thin aluminum layer, the photoresist was stripped. Unfortunately, all metalization again lifted off. The substrate surface was judged to be sufficiently contaminated that further lift-off attempts would prove fruitless. Sample #15 was the last available device-sized $LiNbO_3$ substrate at this late stage of the project period.

Despite the inability to fabricate the electrode structure, tests were performed to verify the optical guiding properties of device #15. The end faces were polished and, using the now familiar test setup, the light focused into the end of the input channel appeared as a bright pinpoint at the termination of the output channel for the guided polarization. Thus, the device was at least partially transmitting in the unbiased state. To test the functioning of the 3 guide couplers, the substrate was sawed in two transverse to the propagation direction in the central branched section. This new end face was polished, and again using the test set up, two pinpoints of light could be observed at the two channel terminations at the output face edge for the guided polarization.

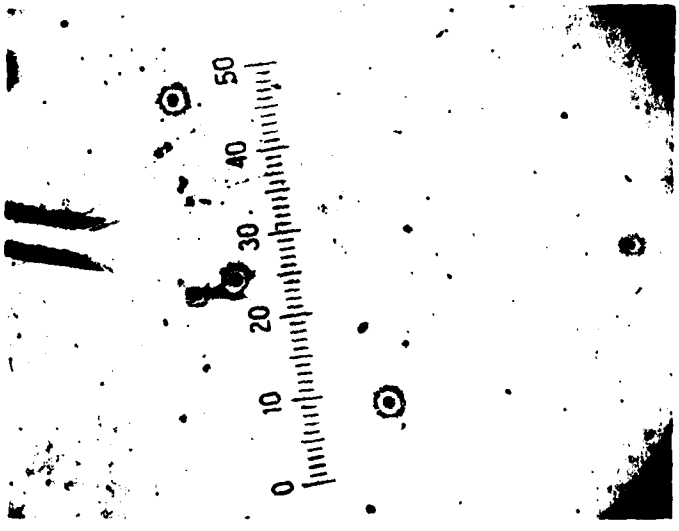

Figure 7

Although the asymmetric PSCL could not be fabricated on device #15 by the liftoff technique, it was still possible to make this microwave line on a clean blank of $LiNbO_3$ using positive photoresist and an etch technique. Some tests of the microwave line performances were then made in the absence of a guided optical signal, as described below.

The asymmetric PSCL was produced by the photolithographically masked etch of 1200Å Aluminum on a clean polished $LiNbO_3$ blank. The metal thickness was measured by interference microscope. The measured dc resistance of the line was 11 ohms, somewhat higher than expected. This has been attributed to the very thin metal layer thickness and to a fabrication flaw which caused the conducting strip to narrow at one point. The line was tapered with fixed ratio of strip width and gap towards the input and output ends for easier connection with the input and output coaxial cables (semirigid .085 inch). The coaxial lines were supported by a brass block, which rested on the ground plane electrode. The input VSWR was less than 1.8 in the frequency range of the test equipment, .5 MHz to 1.3 GHz.† The real criterion for the performance of the asymmetric PSCL in an integrated optical modulator is not how well matched it is to the rest of the system, but how efficiently the applied voltage modulates the light. This can only be measured by the modulation effects themselves. Unfortunately, without a successful device this proved to be impossible within the limits of the project period.

---

†Our calculations estimated a bandwidth of approximately 8 GHz for this device.

IV. CONCLUSION

Within this project, active efforts were made to develop novel means of design and fabrication of wide bandwidth optical channel waveguide switch modulators. In particular, we were led to consider an integrated Mach-Zehnder interferometer (balanced optical bridge) in which wideband electrooptic electrical signals were synchronously applied through an axisymmetric coplanar waveguide electrode structure. Our design calculations show that such an arrangement is of considerable merit in high speed switching of channel waveguides based on optical materials which possess moderate-to-small dielectric constants. While several of the device components were successfully fabricated in the laboratory we were unable to complete the construction of a fully working $LiNbO_3$-based device within the limits of the project period. Many useful lessons were nevertheless learned regarding the fabrication of integrated optical devices with relatively modest equipment and cost.

References

[1] L. Goldberg and C. Lee, Rad. Sci. 12, 537 (1977)

[2] R. V. Schmidt and H. Kogelnik, Appl. Phys. Lett. 28, 503 (1976)

[3] H. Kogelnik and R. V. Schmidt, IEEE J. Quant. El. QE-12, 396 (1976)
V. Ramaswamy and R. D. Standley, Bell System Tech. J. 55, 767 (1976)

[4] C. P. Wen, IEEE MTT-17, 1087 (1969)

[5] M. Izutsu, Y. Yamane, and T. Sueta, IEEE J. Quant. El. QE-13, 287 (1977)
and M. Izutsu et. al. IEEE J. Quant. El. QE-14, 394 (1978)

[6] E. A. J. Marcatili, Bell System Tech. J. 48, 2071 (1969)

[7] I. P. Kaminow and L. W. Stulz, Appl. Phys. Lett. 33, 62 (1978)

[8] P. Cross and R. V. Schmidt, IEEE J. Quant. El. QE-14, 648 (1978)

[9] K. Iwasaki, S. Kurazono, and K. Itakura, Electr. and Comm. in Japan 58-C, 100 (1975)